Making 802.11 DCF Near-Optimal: Design, Implementation, and Evaluation

Jinsung Lee, Hojin Lee, Yung Yi and Song Chong
EE Dept., KAIST, Korea

Bruno Nardelli
ECE Dept., Rice Univ.
Houston, TX, USA

Mung Chiang
EE Dept., Princeton Univ.
Princeton, NJ, USA

***Abstract*—This paper proposes a new wireless MAC protocol called *Optimal DCF* (O-DCF). O-DCF modifies the rule of adapting CSMA parameters, such as backoff time and transmission length, based on a function of the supply-demand differential captured by the local queue length. O-DCF is fully compatible with 802.11 hardware, so that it can be easily implemented only with a simple device driver update. O-DCF is inspired by the recent theoretical studies on queue-based CSMA for high throughput and fairness. O-DCF effectively bridges the gap between theory and practice, implemented and tested in an off-the-shelf 802.11 chipset. Through extensive simulations and real experiments with a 16-node wireless network testbed, we evaluate the performance of O-DCF and show that it outperforms other competitive ones, such as 802.11 DCF, optimal CSMA, and DiffQ for various scenarios.**

I. Introduction

Extensive research documents poor coordination of the standard 802.11 DCF for jointly providing efficiency and fairness, and suggests ways to improve it. Some proposals take a clean-slate approach to redesign CSMA. In the theory community, achieving optimal performance (throughout and/or fairness) in CSMA can sometimes be proved under idealized assumptions such as no collision or perfect synchronization. Other solutions are constrained to operate over legacy 802.11 hardware with only a device driver update, but their performance improvements are often marginal. Among prior works to improve 802.11 DCF is the seemingly conflicting pair of random access philosophies: In face of collisions, should transmitters become more aggressive given that the supply of service rate may become lower than the demand (as in the recently developed theory of Optimal CSMA (oCSMA), e.g., [1]–[5])? Or should they become less aggressive given that collisions signal a contentious RF environment (as in a typical exponential backoff in 802.11 DCF)?

In this paper, we propose a new wireless MAC protocol, called *Optimal DCF* (O-DCF),[1] showing that the two approaches are in fact complementary, where the best combination depends on the logical contention topology, but can be learned without knowing the topology. O-DCF is inspired on the ideas of CSMA adaptation developed by different analytical optimization work [1]–[5], but it is designed to (i) be fully compatible with off-the-shelf 802.11 chipsets, and (ii) achieve high performance in practice by tackling practical issues encountered in actual deployment, which are largely ignored in theory, yet have high impact on actual performance.

[1]We just use the word 'optimal' because our protocol is inspired in part by the recent CSMA theory, called optimal CSMA.

In O-DCF, a product of access probability (determined by contention window (CW) size in 802.11) and transmission length is set to be proportional to the supply-demand differential for long-term throughput fairness. Towards the goal of achieving high performance in practice, a good combination of access probability and transmission length is taken, where such a good access probability is "searched" by Binary Exponential Backoff (BEB) in a fully distributed manner to adapt to the contention levels in the neighborhood. Then, transmission length is suitably selected for long-term throughput fairness. Thus, BEB is exploited not just to conservatively respond to temporal collisions, as in the standard 802.11, but also to be adapted to appropriate access aggressiveness for high fairness and throughput by being coupled with the transmission length.

We first summarize three key design ideas of O-DCF:

D1. Link access aggressiveness is controlled by both CW size and transmission length, based on per-neighbor local queue length at MAC layer, where the queue length quantifies supply-demand differential. Links with bigger differential (i.e., more queue buildup) are prioritized in media access by decreasing CW size and/or increasing transmission length.

D2. The CW size and transmission length are adapted in a fully distributed manner, depending on network topology that affects contention patterns in the neighborhood. Each link first chooses the initial CW size as a decreasing function of the local queue length and increases the CW size against collisions (i.e., BEB). Then, transmission length is decided by a "smart" combination of the resulting CW size (at which transmission succeeds) and the local backlog.

D3. When wireless channels are heterogeneous across links, e.g., a 2Mbps link and another 6Mbps link, the link capacity information is reflected in controlling access aggressiveness by scaling the queue length proportionally to the link capacity. This adaptive control based on link capacity ensures better fairness and higher throughput, since links with better channel condition are scheduled more than those with poor channel condition.

The key design ideas mentioned above are implemented through the following protocol mechanisms:

P1. Each transmitter maintains two queues for each neighbor, referred to as Control Queue (CQ) and Media Access Queue (MAQ). CQ buffers the packets (from the upper-layer) which are dequeued into MAQ. The length of MAQ refers to the local queue length in ***D2***, determining access aggressiveness by adjusting CW size and transmission length. The dequeue rate from CQ to MAQ is controlled through the MAQ length to ensure various, tunable fairness criteria and high throughput.

P2. Once the initial CW size is chosen as a function of the length of MAQ, BEB "searches" for the CW size at which transmission becomes successful in a fully distributed manner. This successful CW size is used to choose the transmission length as described in ***D2***.

P3. We adapt transmission length based on time rather than bytes to achieve time fairness even under heterogeneous channels. To that end, we exploit instantaneous link information from the rate-adaptation module in the 802.11 driver to determine the proper number of bytes to send, according to modulation and coding rate in use.

All of the above mechanisms can be implemented using unmodified 802.11 chips, as we have done in evaluating O-DCF over a 16-node wireless testbed. In particular, the mechanisms satisfy the following constraints of operation over 802.11: First, 802.11 hardware uses a single queue (called Interface Queue (IQ)) shared by all local flows, so that neighbor-specific packet control necessitates additional queues such as CQ and MAQ on top of the IQ. Second, CW values are allowed by only some powers of two and thus we can only choose a value from the set $\{2^n - 1 : n = 1, \cdots, 10\}$. Third, the transmission length is bounded by some value that depends on the 802.11 chipset. For chipsets supporting packet aggregation, it is constrained by some predefined number. [2]

To evaluate the performance of O-DCF, we have implemented O-DCF on a 16-node wireless testbed as well as a simulator for large-scale scenarios that are difficult to be configured in the real testbed. By comparing O-DCF with 802.11 DCF, two versions of oCSMA, and DiffQ [7], we observe that in presence of conditions that are known to be critical to other CSMA protocols, O-DCF achieves near-optimal fairness among flows, with up to 87.1% fairness gain over 802.11 DCF.

II. Related Work

Numerous papers have reported the performance problems of 802.11 DCF, and proposed many solutions to them. To name just a few, 802.11 DCF has severe performance degradation and throughput disparities among contending flows in the topologies such as hidden-terminal (HT), information asymmetry (IA), flow-in-the-middle (FIM), and packet capture [8]–[11], and heterogeneous link capacities [12]. We classify the solution proposals into the efforts at MAC and/or PHY. Some papers proposed new access methods such as dynamic adjustment of CW under 802.11 DCF, e.g., [13], [14] and there exist the implementation researches along this line, e.g., [15], [16]. Other work presented efficient aggregation schemes and their real implementations for throughput improvement, e.g., [17], [18]. Note that most implementations mentioned above individually focused on some specific topologies such as fully-connected (FC) case, and do not explicitly consider problematic ones such as HT, IA, and FIM. With the aid of PHY-layer, there are totally novel approaches, e.g., [19], [20]. This kind of work exploits more information from PHY layer and/or applies new PHY technologies thus not at the MAC layer. In O-DCF, we extend MAC-level operation *by controlling the CW size as well as the transmission length based on the supply-demand differential*. The PHY-layer based approach is to a certain extent orthogonal to our approach, which even can be integrated with O-DCF for further performance improvement.

Recently, analytical studies proved that, under certain assumptions, queue-length based scheduling via CSMA can achieve maximum throughput and/or fairness without message passing e.g., [1]–[3], which is referred to as oCSMA in this paper. Moreover, multiple theoretical papers presented solutions based on the similar mathematical framework, each of them focusing on different aspects of the protocol operation [4], [5]. See [21] for a survey. Our work is in part motivated by oCSMA theory, but as reported in [22], [23] and our evaluation, there still exist many gaps between oCSMA theory and 802.11 practice. [7], [24], [25] bridge the gaps between theory on queue-based MAC (not necessarily CSMA) and practice by reflecting queue length over 802.11. In [7], the authors implemented a heuristic differential backlog algorithm (DiffQ) over 802.11e. EZ-Flow was proposed to solve instability due to large queue buildup in 802.11 mesh networks [24]. Recently, the authors in [25] implemented a backpressure scheduling based on TDMA MAC, which operates in a centralized way. In contrast with the aforementioned work, we present the first asynchronous CSMA based protocol, motivated by optimal CSMA theory and designed to work on top of legacy 802.11 hardware, that can attain high performance even in several adverse scenarios.

III. How Does O-DCF Work?

A. Balancing Supply-Demand Differential

In 802.11 DCF, packets from the upper-layer are enqueued to IQ at 802.11 chip for media access. In O-DCF, we additionally maintain two per-neighbor queues (CQ and MAQ) over IQ, to balance the link's supply and demand through fair media access, as shown in Fig. 1. Denote by $Q_l^C(t)$ and $Q_l^M(t)$ the lengths of CQ and MAQ for each link l at time t. We further maintain a variable $q_l^M(t)$, which is simply the scaled version of $Q_l^M(t)$, i.e., $q_l^M(t) = bQ_l^M(t)$, where b is some small value.[3] Finally, the value of $Q_l^M(t)$ is crucial in O-DCF in that both the dequeue rate from CQ to MAQ and the aggressiveness of media access tightly rely on $Q_l^M(t)$.

First, we control the dequeue rate from CQ to MAQ (when CQ is non-empty), such that it is inversely proportional to $q_l^M(t)$, by $V/q_l^M(t)$,[4] where V is some constant controlling the sensitivity of the dequeue rate to MAQ. Second, in terms of aggressiveness in media access, an initial CW size and transmission length, which determine the dequeue rate of MAQ, is set as a function of $q_l^M(t)$ (see Sections III-B and III-C for

[2]For example, it is determined by the minimum of maximum allowable time and maximum aggregation size, e.g., 10 ms and 64 KB in 802.11n [6].

[3]The value b is referred to as a step size in theory, which is used to slow down the variation of queue lengths, as well as to have feasible CW sizes in the aggressiveness update, see Remark 5.1.

[4]This form of injection pattern is for achieving proportional fairness. However, as will be explained in Section IV-A, this can be changed towards other fairness criterion.

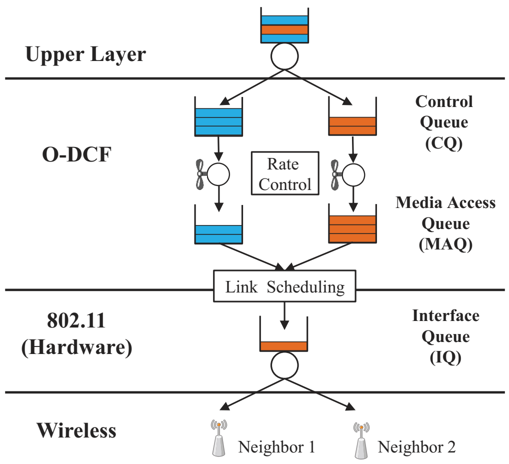

Fig. 1. Queue structure of O-DCF.

details). Then, whenever a new arrival from CQ or a service (i.e., packet transmission) from successful media access occurs, $Q^M(t)$ is updated by:

$$Q_l^M(t+\delta t) = \big[Q_l^M(t) + \big(\text{arrival from CQ} - \text{service from MAQ}\big)\big]_{Q_{\min}}^{Q_{\max}}, \quad (1)$$

where δt is the elapsed time of the next arrival or service event after t. The service from MAQ occurs when the HOL (Head-Of-Line) packet of MAQ is moved into IQ. For multiple neighbors, the largest MAQ is served first; If the chosen transmission length exceeds a single packet size, multiple packets from the same MAQ are scheduled in succession. $Q_{\max}$ is the physical buffer limit of MAQ, but $Q_{\min}$ is set as a small positive value to prevent impractically high injection rate from CQ to MAQ, when $Q_l^M(t)$ (and thus $q_l^M(t)$) approaches zero.

B. Initial CW with BEB

When a link l is scheduled at time t, its initial CW size ($CW_l(t)$) and the number of bytes to transmit ($\mu(t)$) are set adaptively as a function of the length of MAQ. First, $\mu(t)$-byte transmission over l is assigned with the following CW size:

$$CW_l(t) = \frac{2\big(\exp(q_l^M(t)) + C\big)}{\exp(q_l^M(t))} - 1, \quad (2)$$

where C is some constant whose suitable value will be discussed in Section IV-B. We want to use $CW_l(t)$ as the minimum CW ($CW_{\min}$) in 802.11 DCF. But since the 802.11 hardware only allows CW values as powers of two, We use one of possible values closest to (2) as $CW_{\min}$. Then, the media access is attempted after the time (in mini-slots) randomly chosen from the interval $[0, CW_{\min}]$. Intuitively, we assign higher aggressiveness in media access for larger MAQ size, remarking that (2) is decreasing with $q_l^M(t)$. Whenever collision happens, this CW value increases exponentially by BEB. In Section IV-B, we will explain that BEB is not just a component often constrained by some legacy 802.11 hardware,[5] but is an important component to choose an appropriate access aggressiveness and reduce collisions inside our design rationale in a distributed manner.

It is often convenient to interpret CW_l with its corresponding access probability p_l using the relation $p_l = 2/(CW_l+1)$ [13], [14], where the initial CW_l selection in (2) is regarded as the following *sigmoid* function:

$$p_l(t) = \frac{\exp(q_l^M(t))}{\exp(q_l^M(t)) + C}. \quad (3)$$

We delay our discussion on why and how this sigmoidal type function helps and what choice of C is appropriate to Section IV-B.

C. Transmission Length Selection

Our method for the adaptation of the transmission length $\mu_l(t)$ upon channel access by link l is to set $\mu_l(t)$ as a function of the success access probability (equivalently, the success CW size) and the size of MAQ (i.e., $Q_l^M(t)$). Again, by the success CW size, we mean that the transmission becomes successful at that CW size, which is often larger than the initial CW size due to BEB. The rationale to search for the success CW size lies in the fact that it is the actual value used in media access for successful transmission. However, it usually requires quite high overhead for the device driver to read such a success CW size in real-time, which may result in delaying packet scheduling. Thus, we estimate it based on the equation [27] which describes the connection between the initial CW (CW_l), collision ratio (p_c), and the success access probability after BEB (denoted by $\tilde{p}_l$), given by:

$$\tilde{p}_l = \frac{2q(1-p_c^{m+1})}{(CW_l+1)(1-(2p_c)^{m+1})(1-p_c) + q(1-p_c^{m+1})}, \quad (4)$$

where $q = 1 - 2p_c$ and m is the maximum retransmission limit. The collision ratio p_c can be computed for arbitrary topologies [9], only if nodes have the complete knowledge of topology via message passing. To avoid such message passing, we measure the packet collisions by counting the number of unacked packets and normalizing them. Using $\tilde{p}_l(t)$, in O-DCF, the transmission length (in mini-slots) is chosen by:

$$\mu_l(t) = \min\left(\frac{\exp(q_l^M(t))}{\tilde{p}_l(t)}, \bar{\mu}\right), \quad (5)$$

where $\bar{\mu}$ is the maximum transmission length (e.g., 64 KB and 10 ms as mentioned earlier, in order to ensure the minimum short-term fairness and prevent channel monopolization by some node). Then, we convert the transmission length in the unit of mini-slots of the 802.11 chipset into that in bytes to compute the number of packets for aggregate transmission by μ_l (bytes) $= \mu_l$ (slots) $\times C_l$ (Mb/s) $\times t_{\text{slot}}$ (μs/slot), where C_l is the link capacity and t_{slot} is the duration of a mini-slot (e.g., $9\mu s$ in 802.11a). When only a part of μ_l bytes is transmitted due to packetization, we maintain a *deficit counter* to store the remaining bytes of the transmission length that will be used in the next transmission.

D. Channel Heterogeneity and Imperfect Sensing

In practice, wireless channels are heterogeneous across users as well as often time-varying. In such environments, most

[5]In literature, e.g., [26], it is known that BEB can be disabled by using TXQ descriptor in the device driver, which, however, does not work in our chipset, confirmed via our kernel level measurement.

802.11 hardware exploits multi-rate capability of the PHY layer to adapt their rate, e.g., SampleRate [28]. However, it is known that 802.11 DCF is incapable of utilizing this opportunistic feature, leading to the waste of resource called *performance anomaly* [12]. In other words, 802.11 DCF provides equal chances to links (on average), in which case low-rate links would occupy more time than high-rate ones, so that the performance degrades. To provide fairness focusing on time shares instead of rate shares, namely *time-fairness* [29], we slightly modify our rules in selecting the initial access probability as well as the transmission length by replacing $\exp(q_l^M(t))$ with $\exp(c_l(t)q_l^M(t))$ in (2) and (5), where $c_l(t)$ is (relative) link capacity of link l at time t, as theoretically verified by [30]. For imperfect sensing cases such as HT and IA scenarios, we also propose to use a virtual carrier sensing via RTS/CTS signaling, as suggested in literature. In O-DCF, unlike in the standard 802.11a/b/g, RTS/CTS signaling is conducted only for the first packet within the transmission length.

IV. Why Does O-DCF Work?

A. Transferring from Theory to Practice

O-DCF is in part motivated by the recent research on queue-based MAC scheduling in theory community, see e.g., a survey [31] and in particular, so-called oCSMA [1]–[5]. oCSMA is characterized as a variant of CSMA that has a specific rule of setting backoff time and transmission length. The papers in literature are slightly different in terms of the models and conditions, e.g., discrete/continuous, synchronous/asynchronous, or saturated/unsaturated traffic. However, the key idea is largely shared; the queue maintains the supply-demand differential, and the access aggressiveness is controlled by the queue length, which, in turn, depends on the demand (arrival) and the supply (transmission success), formally $p_l(t) \times \mu_l(t) = \exp(q_l(t))$. Together with this parameter control, the source rate control by $U'^{-1}(q(t)/V)$, where $U(\cdot)$ is an utility function, ensures that the long-term throughput is the solution of NUM (network utility maximization). By suitably choosing the form of the utility function, we can achieve various fairness criteria. In this paper, we focus on $U(\cdot) = \log(\cdot)$ (thus, $U'^{-1}(q(t)/V) = V/q(t)$).

We highlight that O-DCF is not just a naive implementation of oCSMA, because (i) many assumptions in the oCSMA theory, e.g., no collisions in the continuous time framework, symmetric sensing, perfect channel holding and etc. do not hold in practice. (ii) Furthermore, O-DCF is constrained to be fully compatible with 802.11 chipsets. (iii) More importantly, in theory, any combination of p_l and μ_l works well as long as their product is $\exp(q_l)$. However, we need to find a careful combination of them for high performance in practice. All of these issues will be elaborated in the following sections.

B. Tension between Symmetric and Asymmetric Contention

(a) Topological dependence. A good combination of two CSMA operational parameters for high performance depends on contention topologies. O-DCF is designed to *autonomously* choose the combination of access probability and transmission length without explicit knowledge of topological information. Just for ease of explanation, we provide our description, assuming that flows are configured in either of the two "extreme" topologies: fully-connected (FC) for symmetric contention and flow-in-the-middle (FIM) for asymmetric contention (see Fig. 2), but O-DCF generally works well beyond these two topologies. Recall the two key design ideas of O-DCF: we first choose the initial access probability as a sigmoid function of the queue length and then let it experience BEB. To summarize, BEB is a key component in symmetric contention and the sigmoid function based access probability selection is crucial in asymmetric contention, and both are important in "mixture" topologies (all of which are presented below, respectively).

(a) FC (b) FIM

Fig. 2. Example topologies' conflicting graphs. Vertices are the links in interference graphs; dotted lines represent interference; (a) FC with 4 links; (b) FIM with 2 outer links.

(b) O-DCF: How exponential backoff helps. In symmetric contention, the access probabilities among contending flows should be reasonably low; otherwise, throughput will naturally degrade. Note that to guarantee fairness and high (long-term) throughput, a tiny p_l can work as it leads to almost no collision. This is because in that case a significantly long transmission length would recover the long-term throughput, as explained in oCSMA theory. However, such a combination will lead to a serious problem in short-term fairness, where a maximum bound on transmission length to guarantee short-term fairness is enforced in practice. For an automatic adaptation to contention level, we utilize BEB as *a fully distributed search process* for the *largest* access probability (i.e., the smallest CW size) that lets the links share the media efficiently in presence of collisions.

(c) O-DCF: Why sigmoid function? As opposed to symmetric contention, in asymmetric contention such as FIM-like topologies, almost no collision occurs and thus BEB rarely operates. More importantly, in this case, the starvation of the central flow is a major issue. To tackle this, we require that the CW size (or the access probability) of link l that solely contends with many other links should be *small (or high)* and thus *prioritized* enough that the link l avoids rare channel access and even starvation. To provide such an *access differentiation*, we focus on the fact that the flow in the middle, say l, typically has a longer queue than the outer flows. Let us denote the access probability p_l by some function of queue length q_l, i.e., $p_l = f(q_l)$. Thus, it is natural to design $f(q_l)$ to be *increasing* for access differentiation.

The question is what form of the function $f(q_l)$ is appropriate for high performance. To better organize the explanation, we first discuss the case with the access probability, and then the CW. Toward efficient access differentiation, we start by the f's requirements: for any link l and for $q_{\min} \le q \le q_{\max}$,

R1: $0 < f(q_l) \le \bar{p} < 1$, where $f(q_{\min}) \approx 0$ and $f(q_{\max}) = \bar{p}$. The largest access probability $\bar{p}$ should be strictly less than one to prevent channel monopolization.

R2: $[f(q_l)]_2$ [6] should span all the values in $\{1/2^i : i = 0, \ldots, 9\}$ each of which corresponds to the CW sizes

[6] We denote by $[x]_2$ the $1/2^i$ for some integer i, which is closest to x, e.g., $[0.124]_2 = 1/2^3$ and $i = 3$.

$\{2^{i+1}-1 : i = 0, \ldots, 9\}$.

R3: The transmission lengths of the flows with heavy contention and those with light contention should be kept small not to exceed maximum aggregation size/time.

The requirement ***R3*** is important to prevent the central flow from being starved. In the FIM-like topologies, the flows experiencing heavy contention such as the central one in FIM has very rare chances to access the media. To guarantee (proportional) fairness, it is necessary for such flows to select long transmission lengths whenever holding the channel. However, as mentioned earlier, the transmission length should be bounded with the maximum aggregation size and time for practical purposes such as short-term fairness. This implies that the central flow often needs to stop the transmissions before its required transmission length for optimal fairness is reached. Efficient flow differentiation, which prioritizes the flows with heavy contention in terms of access probability, significantly helps by reducing the required transmission length with a reasonable value (mostly shorter than the maximum transmission length) towards long-term fairness. An extreme case for asymmetric contention is an IA scenario where two flows have asymmetric interference relationship. We will explain in Section IV-C that our flow differentiation helps a lot in providing (long-term) fairness in such a problematic scenario.

An intuitive way to realize flow differentiation is to set the access probability of link l to be $\exp(q_l)/K$ for some constant K. Then, the rule (5) enforces the transmission length to be around K, *irrespective of the contention levels of the flows* (i.e., ***R3***). However, to satisfy ***R1***, we use a slightly different function that has a sigmoidal form, $f(q_l) = \frac{\exp(q_l)}{\exp(q_l)+C}$, with some constant C. This function naturally makes the chosen access probability to be strictly less than one for any q_l such that $q_{\min} \leq q_l \leq q_{\max}$, unlike $\exp(q_l)/K$. Clearly, the sigmoid function is not exponential over the entire $q_{\min} \leq q_l \leq q_{\max}$ values. However, it suffices to have an exponential form up to q'_l with $f(q'_l) = 0.75$, since for a larger $q_l > q'_l$, the CW size approaches one from the CW granularity (but, the access probability is set to be strictly less than one).

Then, the next question is the inflection point, determined by the constant C. We choose C around 500 due to the following reasons. First, for the resultant p to span the whole feasible values (as in ***R2***), C should be greater than 500, i.e., $f(q_{\min}) = \frac{\exp(q_{\min})}{\exp(q_{\min})+500} \approx \frac{1}{512}$, where $q_{\min} = bQ_{\min} = 0.01$ (see Fig. 3(b) in terms of CW). Second, the parameter C determines the location of inflection point in the sigmoid function. For example, let us consider the FIM topology with four outer flows, where the central flow can have its queue length of up to five, while the outer flows have much smaller queue lengths usually less than two. To guarantee the exponential increase in that curve, the x-axis at the inflection point should be larger than five, implying that C larger than 500 is sufficient since $f(5) = \frac{\exp(5)}{\exp(5)+500} < \frac{1}{2}$. However, too large C values directly result in too long transmission lengths from (5) because they may yield very low p's.

(d) Mixture of contention levels. In practice, it is possible for a link to appear in a mixture of topologies with symmetric and asymmetric contention. We study this issue using the example

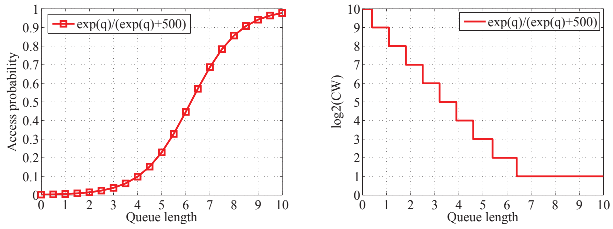

(a) Queue vs. p (b) Queue vs. CW

Fig. 3. Illustration of sigmoid function with respect to queue length.

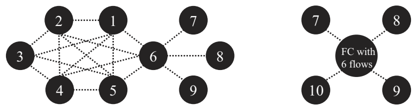

(a) FIM with FC (b) FC in FIM

Fig. 4. Mixed topologies' conflicting graphs; (a) The flow 6 belongs to both FC and FIM topologies; (b) six flows within a FC group form a FIM topology with four outer flows.

scenarios in Fig. 4. First, in Fig. 4(a), flow 6 interferes with flows 1, ..., 5 in a fully-connected fashion, and also with flows 7, 8, and 9 in a FIM-like fashion. Since it senses the transmission of both the remaining links forming the FC group and outer links forming the FIM group, its queue temporarily builds up, thus having a larger access probability than outer links due to the sigmoidal curve. However, it shares the medium equally with others in FC group so that their queue lengths increase together. Thus, in the worst case, BEB can prevent too aggressive access among the links within FC group. More importantly, *even the reduced access probability from BEB is kept larger than those of outer links* (see Section V-B for simulation results), thus still being sufficiently prioritized in the FIM topology, preserving proportional fairness. Similar trends are also observed in Fig. 4(b).

(e) Aggressiveness control for session tails. Sessions dynamically enter and leave over time. As sessions' packets are served in a node (without new session arrivals), the CQ size naturally decreases, resulting in progressively less aggressive media access. In O-DCF, as the CQ size becomes zero, we record the MAQ size at that time, and access the media with the recorded MAQ size (not actual MAQ size) until all the packets at MAQ are served. This effectively solves the problem that the session tails may be processed with too low aggressiveness.

C. Imperfect Sensing and Capture Effect

Above, we discussed the performance and operation of O-DCF in low-collision scenarios. However, sensing is often imperfect, as illustrated in Fig. 5. RTS-CTS-like virtual sensing in O-DCF is not a complete solution, because just a naive choice of access probability and transmission length may generate a self-feeding loop where collisions increase queue lengths, which in turn leads to more aggressive access and thus heavier collisions, especially under the CW adaptation (defined in Section V-A) [23]. Our queue based initial CW with BEB substantially lessens such bad impacts. In *HT*, if the queue lengths of hidden nodes are large, BEB lets each node increase its CW, so that with small time cost, a transmission succeeds. This successful transmission generally decreases the queue lengths, preventing CW from being too small due to queue

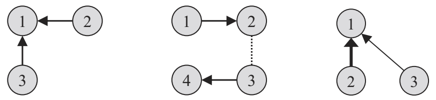

(a) HT (b) IA (c) HT with capture.

Fig. 5. Example topologies of imperfect sensing and packet capture. In network graphs, vertices represent nodes, dotted lines represent connectivity, and arrows represent flows. (a) HT; (b) IA; (c) HT with capture: a thin arrow for weak signal.

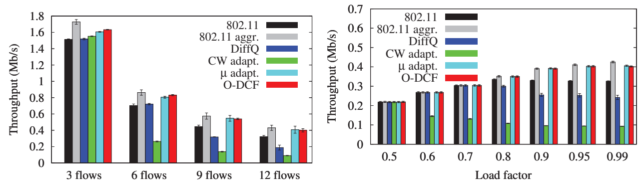

(a) Per-flow throughput (b) System throughput

Fig. 6. (a) Average throughput in FC with 3, 6, 9, and 12 fully-backlogged flows (b) System throughput for dynamic traffic.

based initial CW selection. In *IA*, collisions are asymmetric. Suppose that at some time, advantaged and disadvantaged flows have small and large queue lengths, respectively. Then, the disadvantaged flow will have a smaller initial CW, thus leading to successful transmissions and simultaneously the advantaged flows will hear CTS signalling (responding to RTS from the disadvantaged flow) and stop their attempts. This helps a lot in providing fairness between two asymmetric flows. The packet capture effects can be handled by our method similarly to the IA scenario, i.e., interference asymmetry. For example, in *HT with capture,* similar behaviors to the IA case occur between weak and strong nodes.

D. O-DCF Implementation

(a) Queue structure. We implemented O-DCF as an overlay MAC on legacy 802.11 hardware using our C-based software platform, which requires protocol implementation on top of MadWiFi device driver [32]. Due to a limited memory size of legacy network interface card (NIC), we implement CQ and MAQ at the user space level. Note that the scheduling from MAQ to IQ is not an actual packet transmission to the media. To minimize the temporal gap between the service from MAQ and the actual transmission, we reduce the buffer limit of IQ to one through a device driver modification.

(b) O-DCF scheduler and parameter control. A scheduler in O-DCF schedules packets enqueued at MAQ to send them into the 802.11 hardware, as shown in Fig. 1. Whenever IQ in 802.11 becomes empty, the scheduler in O-DCF is notified by a system call such as `raw socket` function and determines the next packet to be enqueued into IQ, by comparing the lengths of multiple per-neighbor MAQs. Meanwhile, the scheduler maintains CSMA parameters, such as CW, AIFS, and NAV values, for each MAQ's HOL (Head-Of-Line) packet. To facilitate packet-by-packet parameter control, we piggyback such parameters into the header of HOL packet, so that the modified driver can interpret and set them in the TXQ descriptor of an outgoing packet for the actual transmission.

(c) Long data transmission. When packet aggregation is not supported in legacy 802.11 hardware, as in our real testbed, such as 802.11a/b/g, we take the following approach. The O-DCF scheduler assigns different arbitration inter-frame spaces (AIFSs) and CWs for packets inside the specified transmission length. Since AIFS defines a default interval between packet transmissions and the smallest CW indicates the shortest back-off time, this provides a prioritization for *back-to-back* transmissions until the given transmission length expires. Further, we exploit the network allocation vector (NAV) option that includes the time during which neighbors remain silent irrespective of sensing. This guarantees that even interfering neighbors unable to sense (due to, e.g., channel fluctuations) do not prevent the transmission during the reserved transmission length.

V. Performance Evaluation

A. Setup

We use both NS-3 simulations and real experiments on a 16-node wireless testbed. The simulations are conducted for basic topologies as well as topologies that are hard to manually configure in real experiments. We perform testbed experiments for spontaneous deployment in a building as well as topologies that are more sensitive to the real effects such as packet capture. The details of our testbed specification will be described in Section V-C. For all scenarios, we execute ten runs (each lasting for 100 seconds) and measure the goodput at receiver, and the length of error bars in all plots represents standard deviation. The packet size is 1000 bytes. The parameters used in O-DCF are as follows: the queue scaling constant $b = 0.01$, the queue bounds are $Q_{\min} = 1$, $Q_{\max} = 1000$, and $V = 400$ (recall that the dequeue rate from CQ to MAQ is $V/q_l^M(t)$). We consider fully-backlogged flows in most scenarios, except when evaluating how O-DCF works for dynamic session arrival and departure. See Remark 5.1 for our parameter choices and other evaluation results.

We compare (i) 802.11 DCF with/without frame aggregation, (ii) two versions of oCSMA in theory, and (iii) DiffQ [7]. In 802.11 with frame aggregation, we set the size of frame aggregation to three packets, which is equivalent to the average transmission length in O-DCF. Since our testbed is based on 802.11a (which does not support frame aggregation), we include 802.11 with frame aggregation only in simulations. For the standard oCSMA, we test two versions to show the effect of our automatic CSMA parameter combination in O-DCF: (a) *CW adaptation* in which we typically fix the transmission length μ with a single packet and control the access probability $p_l(t)$, such that $p_l(t) \times \mu = \exp(q_l(t))$ [1], and (b) *μ adaptation with BEB* (simply μ adaptation in this paper) in which we delegate the selection of $p_l(t)$ to 802.11 DCF and control $\mu_l(t) = \exp(q_l(t))/p_l(t)$. Note that to understand the effect of different methods for the adaptation of CWs, we evaluate μ adaptation with BEB using 802.11's CW size, and compare it with O-DCF. DiffQ is a *heuristic* harnessing the 802.11e feature, and schedules the interfering links with different priorities based on queue lengths.

B. Simulation Results: Basic Topologies

(a) Fully-connected (FC): Impact of contention degrees. Fig. 6(a) summarizes the average per-flow throughput for the FC topologies (see Fig. 2(a)) for varying contention levels. The

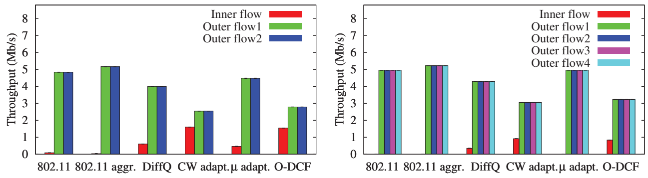

(a) 2 outer flows (b) 4 outer flows

Fig. 7. FIM topology with two and four outer flows. In (a) and (b), the ideal proportional-fair throughput ratios of an outer flow and a middle flow are: 2:1 and 4:1, respectively.

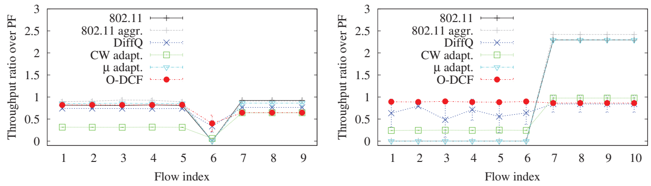

(a) FIM with FC (9 flows) (b) FC in FIM (10 flows)

Fig. 8. Simulation. Performance comparison in two mixed topologies; the flow indexes are the same as in Fig. 4; we plot the throughput ratio over optimality: the closer to one the ratio is, the better fairness is.

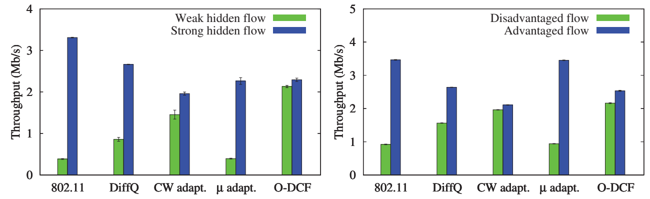

(a) HT w/ cap. (b) IA

Fig. 9. Performance comparison in HT with packet capture (left) and IA (right) topologies.

main message here is that O-DCF exhibits efficiency comparable to 802.11 for varying contention levels. All algorithms are good for the small number of flows. However, with increasing contention levels, the throughputs of CW adaptation and DiffQ decrease significantly since high contentions make those two protocols choose too small CW size, leading to frequent collisions. Meanwhile, O-DCF smoothly adapts contention levels by the smart selection of the combinations of transmission length and CW size. We also see the effect of frame aggregation in O-DCF and 802.11 with frame aggregation.

(b) Flow-in-the-middle (FIM): Impact of contention asymmetry. Next, we study the case of asymmetric contention, using the FIM (see Fig. 2(b)). As shown in Fig. 7, O-DCF and CW adaptation dominate other algorithms in terms of fairness. As reported in other papers [7], [9], the central flow experiences serious starvation in 802.11. In contrast to the symmetric contention as in FC, μ adaptation with BEB leads to the starvation of the central flow, since outer flows use 802.11's small CW to access the channel due to few collisions, which is too short to have enough overlapping of silent times and let the central flow transmit. Thus, in O-DCF, we can adapt the transmission length μ with a smarter CW selection method for high fairness. DiffQ resolves the starvation of the central flow well, but it shows suboptimal performance due to the heuristic setting of CW size.

(c) Mixed topologies. We now consider the case when some flows belongs in part to symmetric and asymmetric contention, as in Fig. 4. Fig. 8(a) shows the normalized per-flow throughput by the optimal PF share over the topology in Fig. 4(a). We observe that O-DCF outperforms others in terms of fairness. Note that the flow 6 placed between two different contention patterns experience some suboptimal fairness. This is because flow 6 should have low access probability due to the contention with flows 1-5, but it should also be prioritized over the flows 7-9. Our result show that despite such conflicting situations, O-DCF tries to adjust the access probability and set the transmission length, so that the fairness sustained to be reasonable, whereas other algorithms suffer from bad fairness. Similar principles are applied to the topology in Fig. 4(b), as shown in Fig. 8(b).

(d) Dynamic traffic. In addition, we evaluate the case with bursty traffic where active flow sessions can dynamically arrive or leave the system. In a fully-connected topology with 12 flows, we generate multiple active sessions, each of them transferring a file of 1 MB size. The results are shown in Fig. 6 (b), for different system load values. To obtain different load levels, we vary the session inter-arrival times, which is $1\text{MB}/(5.4\text{ Mb/s} \times \text{load factor}) \times 12$. Then, we evaluate system throughput vs. load as shown in the figure. We observe that, when the network load is low, all protocols can satisfy the flow traffic demands (see the case with load factor 0.5), and therefore all protocols have similar performance. However, as the load in the network increases, the system starts behaving in a more similar way to the fully-backlogged case, accumulating packets at the MAC layer queues as traffic demands overload system capacity. As an extreme case, for a network load of 0.99, we observe a very similar performance for all protocols to the one in Fig. 6a (i.e., the fully-backlogged case). In conclusion, with bursty traffic, low demands are easy to satisfy by any of the protocols, but with bursty traffic and higher demands, the benefits in the use of O-DCF become more evident, and are comparable to the ones already explained for the fully-backlogged case.

C. Experiments

In our 16-node testbed, each node is a netbook platform (1.66 GHz CPU and 1 GB RAM) running Linux kernel 2.6.31 and equipped with a single 802.11a/b/g NIC (Atheros chipset) running the modified MadWiFi driver for O-DCF's operations. To avoid external interference, we select a 5.805 GHz band in 802.11a. The default link capacity is fixed with 6 Mb/s, but we vary capacity or turn on auto rate adjustment, if needed.

(a) Imperfect sensing and capture effect. We investigate the impact of imperfect sensing in O-DCF with the topologies: HT with capture and IA, as depicted in Fig. 5. As discussed in Section IV-C, we enable a virtual sensing, i.e., RTS/CTS signaling by default for better channel reservation in all algorithms. Fig. 9 shows throughputs for HT and IA, respectively. First, in HT with packet capture, O-DCF outperforms others in asymmetric conditions due to packet capture by hidden nodes as well as symmetric conditions (whose result is omitted but can be found in [33]). Specifically, in O-DCF, collisions and thus BEB allow the hidden flows to access the media with larger CWs (i.e., less aggressiveness), resulting in many successful RTS/CTS exchanges. Fairness is supported by the transmission length control. Second, in IA, O-DCF shows fair and high throughput, where the advantaged flow has a larger CW due to

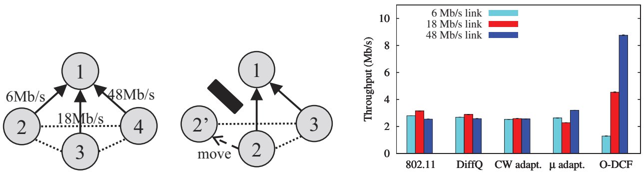

(a) Static case (b) Mobile case (c) Per-flow throughput

Fig. 10. Experiment. Single-hop network scenario consisting of clients and one AP; (a) static case: all nodes remain fixed with different PHY rates; (b) mobile case: node 2 moves away from node 1 at 60 seconds.

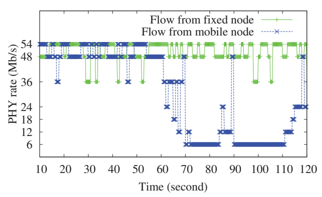

(a) Runtime PHY rate (b) O-DCF w/ rate update

Fig. 11. Experiment. Performance evaluation in mobile scenario (Fig. 10(b)).

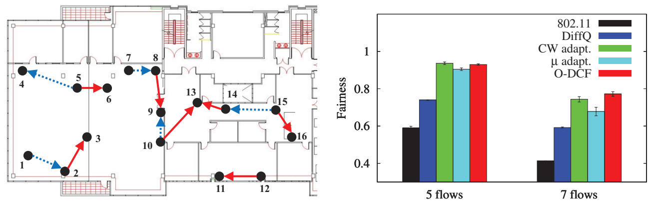

(a) Tested scenario (b) Jain's fairness

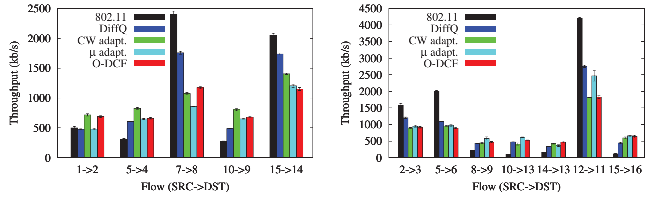

(c) Per-flow throughput of 5 flows (d) Per-flow throughput of 7 flows

Fig. 12. Experiment. Tested topology and performance comparison; (a) 16 nodes denoted by triangles are distributed in the area of 40m x 20m; dotted (solid) arrows represent 5 (7) flows for the first (second) scenario. (b) Jain's fairness comparison. (c)-(d) Per-flow throughput distributions.

small backlogs, and the disadvantaged flow also uses a larger CW due to BEB, responding well to collisions. As a result, both flows contend with sufficiently large CW values without heavy collisions, enjoying better RTS/CTS-based reservation. In μ adaptation, the advantaged flow accesses the channel using 802.11's small CW due to few collisions, which leads to a high probability of collisions and even starvation of the disadvantaged flow, and thus unfairness between two flows deepens. DiffQ cannot solve unfairness perfectly due to the still aggressive CW values. However, CW adaptation grants more aggressiveness to less-served flows, thus reducing the throughput gap between two flows in both scenarios, while still leaving a small gap from optimality.

(b) Heterogeneous channels. We consider two scenarios: (i) *static* in Fig. 10(a): nodes are stationary with different link rates, 6, 18, and 48 Mb/s, and (ii) *mobile* in Fig. 10(b): each node turns on the auto-rate functionality and two clients send their data to a single AP, and after 60 seconds, one of two clients (say node 2) moves away from AP (node 1). In adapting the rate, we employ the SampleRate algorithm [28] in MadWiFi driver. We measure the runtime PHY rate information updated every one second interval. First, in the static scenario, as shown in Fig, 10(c), we observe that only O-DCF can attain proportional fair rate allocation in an efficient manner, because of the consideration of link rate heterogeneity in the choice of CWs and transmission lengths, whereas the other protocols show severe inefficiency that the flows with higher rates are significantly penalized by that with lower rate. Besides the long-term fairness study in the static scenario, we examine the responsiveness of O-DCF to channel variations in the mobile scenario, shown in Fig. 11(a). We trace the instantaneous throughput of both fixed and mobile nodes in Fig. 11(b), where we see that the incorporation of the runtime PHY rate in O-DCF indeed helps in achieving throughput efficiency instantaneously even in the auto-rate enabled environment.

(c) Random topology experiment in a building. We now conduct a more general experiment using a 16-node testbed topology, as shown in Fig. 12(a), where we test two cases of five and seven concurrent flows under the default capacity. This random topology enables us to see how the algorithms perform in the mixture of hidden terminals and heavy contention scenarios including FIM scenarios. Fig. 12(b) compares Jain's fairness achieved by all the algorithms for two scenarios. We find that over all the scenarios, O-DCF outperforms others in terms of fairness (up to 87.1% over 802.11 and 30.3% over DiffQ), while its sum utility is similar with others. The fairness gain can be manifested in the distribution of per-flow throughput, as shown in Fig. 12(c) and Fig. 12(d). O-DCF effectively prioritizes the flows with more contention degree (e.g., flow $10 \rightarrow 9$ forms *flow-in-the-middle* with flows $7 \rightarrow 8$ and $15 \rightarrow 14$) and provides enough transmission chances to highly interfered flows (i.e., $8 \rightarrow 9$, $10 \rightarrow 13$, and $14 \rightarrow 13$), compared with 802.11 DCF and DiffQ. The experimental topology is somewhat limited in size, tending to be full-connected. This leads to a small performance gap between oCSMA and O-DCF, but 802.11 DCF yields severe throughput disparities of more than 40 times between flows $12 \rightarrow 11$ and $10 \rightarrow 13$ in the second scenario. Compared with 802.11, DiffQ performs fairly well in the sense that it prioritizes highly interfered flows. However, its access prioritization is heuristic, so there is still room for improvement compared with O-DCF.

Remark 5.1: First, the parameters of O-DCF are: b, $Q_{\min}$, $Q_{\max}$, and V. The value of b can be chosen by a typical step-size in many of optimization algorithms, say 0.01 or 0.001. The queue bound parameter is important, because $Q_l^M(t)$ is used to determine the injection rate from CQ to MAQ (i.e., $V/(bQ_l^M(t))$, connecting to the media aggressiveness. Thus, $Q_{\min}$ and $Q_{\max}$ are chosen just to avoid too small or large injection rates. Finally, it is intuitive that larger V leads to more sensitive response to the changes of $Q_l^M(t)$. This intuition has been widely formalized in theory that V shows a tradeoff between performance and queueing delay [34]. In [33], we show the results for different values of V, where we actually observe such a tradeoff, but O-DCF's strength is not weakened.

Second, due to space limitation, this paper shows only a limited set of simulation and experimental results. We refer the readers to our technical report [33] for a longer list. Our other results include the simulation for large-scale topologies: We generate two topologies in NS-3: 16-node grid and 30-node random topologies. For both scenarios, we observed that O-DCF shows similar trends to those in this paper. Especially, for large-scale topology simulations, O-DCF enhances fairness up to 41.0% (resp., 29.9%) over 802.11 DCF and 24.0% (resp., 12.6%) over DiffQ in the random (resp., grid) network.

Third, it is not surprising that we observe that long transmissions in O-DCF sometimes increase the inter-TX delay of some flows. However, even in such a case, O-DCF still keeps substantial benefits in terms of long-term fairness. This confirms the results of prior work [3], [22], which has shown a tradeoff between short-term fairness and long-term efficiency in oCSMA algorithms. More importantly, the performance benefits in O-DCF can be found in critical scenarios where other CSMA protocols fail to achieve fairness, as shown in the previous sections.

VI. Concluding Remarks

The major design issues to improve 802.11 DCF are contention window selection and transmission length control against network contention, imperfect sensing, channel heterogeneity, and packet capture without any message passing. We proposed a protocol, called O-DCF, inspired by the recent theory on CSMA to tackle these issues. However, we highlight that our work is not just an implementation of what has been developed in theory, covering many important engineering optimizations that have large impacts on the actual performance and deployment in practice. This paper shows that a combination of effective design ideas and implementation choices can actually let a theory-motivated protocol applicable in practice. We hope that our paper encourages and motivates other follow-up work to further bridge the gap between practice and theory. The O-DCF implementation in NS-3 and our technical report are available online at http://lanada.kaist.ac.kr/ODCF.

Acknowledgement

This work was supported by the Center for Integrated Smart Sensors funded by the Ministry of Education, Science and Technology as Global Frontier Project (CISS-2012M3A6A6054195), and was also supported in part by NSF grant CNS-1126478, NSF grant CNS-1011962, and a grant from Cisco Systems Inc.

References

[1] L. Jiang and J. Walrand, "A distributed CSMA algorithm for throughput and utility maximization in wireless networks," *IEEE/ACM Trans. Netw.*, vol. 18, no. 3, pp. 960–972, Jun. 2010.

[2] S. Rajagopalan, D. Shah, and J. Shin, "Network adiabatic theorem: An efficient randomized protocol for contention resolution," in *Proc. ACM SIGMETRICS*, 2009.

[3] J. Liu, Y. Yi, A. Proutiere, M. Chiang, and H. V. Poor, "Towards utility-optimal random access without message passing," *Wirel. Commu. Mob. Comp.*, vol. 10, no. 1, pp. 115–128, Jan. 2010.

[4] J. Ni, B. Tan, and R. Srikant, "Q-CSMA: Queue-length based CSMA/CA algorithms for achieving maximum throughput and low delay in wireless networks," in *Proc. IEEE INFOCOM*, 2010.

[5] P. Marbach and A. Eryilmaz, "A backlog-based CSMA mechanism to achieve fairness and throughput-optimality in multihop wireless networks," in *Proc. Allerton Conf.*, 2008.

[6] D. Skordoulis, Q. Ni, H.-H. Chen, A. P. Stephens, C. Liu, and A. Jamalipour, "IEEE 802.11n MAC Frame Aggregation Mechanisms for Next-Generation High-Throughput WLANS," *IEEE Wirel. Comm.*, vol. 15, no. 1, pp. 40–47, Feb. 2008.

[7] A. Warrier, S. Janakiraman, S. Ha, and I. Rhee, "DiffQ: Practical differential backlog congestion control for wireless networks," in *Proc. IEEE INFOCOM*, 2009.

[8] V. Bharghavan, A. Demers, S. Shenker, and L. Zhang, "MACAW: A media access protocol for wireless LANs," in *Proc. ACM SIGCOMM*, 1994.

[9] M. Garetto, T. Salonidis, and E. Knightly, "Modeling per-flow throughput and capturing starvation in CSMA multi-hop wireless networks," in *Proc. IEEE INFOCOM*, 2006.

[10] X. Wang and K. Kar, "Throughput modelling and fairness issues in CSMA/CA based ad-hoc networks," in *Proc. IEEE INFOCOM*, 2005.

[11] S.-J. Han, T. Nandagopal, Y. Bejerano, and H.-G. Choi, "Analysis of spatial unfairness in wireless LANs," in *Proc. IEEE INFOCOM*, 2009.

[12] M. Heusse, F. Rousseau, G. Berger-Sabbatel, and A. Duda, "Performance anomaly of 802.11b," in *Proc. IEEE INFOCOM*, 2003.

[13] F. Calì, M. Conti, and E. Gregori, "Dynamic tuning of the IEEE 802.11 protocol to achieve a theoretical throughput limit," *IEEE/ACM Trans. Netw.*, vol. 8, no. 6, pp. 785–799, Dec. 2000.

[14] M. Heusse, F. Rousseau, R. Guillier, and A. Duda, "Idle Sense: an optimal access method for high throughput and fairness in rate diverse wireless LANs," in *Proc. ACM SIGCOMM*, 2005.

[15] V. A. Siris and G. Stamatakis, "Optimal CWmin selection for achieving proportional fairness in multi-rate 802.11e WLANs: test-bed implementation and evaluation," in *Proc. ACM WinTECH*, 2006.

[16] Y. Grunenberger, M. Heusse, F. Rousseau, and A. Duda, "Experience with an implementation of the idle sense wireless access method," in *Proc. ACM CoNEXT*, 2007.

[17] Y. Kim, S. Choi, K. Jang, and H. Hwang, "Throughput enhancement of IEEE 802.11 WLAN via frame aggregation," in *Proc. VTC-Fall*, 2004.

[18] W. Kim, H. K. Wright, and S. M. Nettles, "Improving the performance of multi-hop wireless networks using frame aggregation and broadcast for TCP ACKs," in *Proc. ACM CoNEXT*, 2008.

[19] S. Sen, R. R. Choudhury, and S. Nelakuditi, "CSMA/CN: carrier sense multiple access with collision notification," in *Proc. ACM MobiCom*, 2010.

[20] T. Li, M. K. Han, A. Bhartia, L. Qiu, E. Rozner, Y. Zhang, and B. Zarikoff, "CRMA: collision-resistant multiple access," in *Proc. ACM MobiCom*, 2011.

[21] S.-Y. Yun, Y. Yi, J. Shin, and D. Y. Eun, "Optimal csma: A survey," in *Proc. of IEEE ICCS*, 2012.

[22] J. Lee, J. Lee, Y. Yi, S. Chong, A. Proutiere, and M. Chiang, "Implementing utility-optimal CSMA," in *Proc. Allerton Conf.*, 2009.

[23] B. Nardelli, J. Lee, K. Lee, Y. Yi, S. Chong, E. Knightly, and M. Chiang, "Experimental evaluation of optimal CSMA," in *Proc. IEEE INFOCOM*, 2011.

[24] A. Aziz, D. Starobinski, P. Thiran, and A. Fawal, "EZ-Flow: Removing turbulence in IEEE 802.11 wireless mesh networks without message passing," in *Proc. ACM CoNEXT*, 2009.

[25] R. Laufer, T. Salonidis, H. Lundgren, and P. L. Guyadec, "XPRESS: A cross-layer backpressure architecture for wireless multi-hop networks," in *Proc. ACM MobiCom*, 2011.

[26] A. Sharma and E. M. Belding, "FreeMAC: framework for multi-channel mac development on 802.11 hardware," in *Proc. ACM PRESTO*, 2008.

[27] H. Wu, Y. Peng, K. Long, S. Cheng, and J. Ma, "Performance of reliable transport protocol over IEEE 802.11 wireless LAN: Analysis and enhancement," in *Proc. IEEE INFOCOM*, 2002.

[28] J. C. Bicket, "Bit-rate selection in wireless networks," Master's thesis, MIT, 2005.

[29] G. Tan and J. Guttag, "Time-based fairness improves performance in multi-rate wireless LANs," in *Proc. USENIX*, 2004.

[30] A. Proutiere, Y. Yi, T. Lan, and M. Chiang, "Resource allocation over network dynamics without timescale separation," in *Proc. IEEE INFOCOM*, 2010.

[31] Y. Yi and M. Chiang, *Next-Generation Internet Architectures and Protocols*. Cambridge University Press, 2011, chapter 9: Stochastic network utility maximization and wireless scheduling.

[32] "Multiband Atheros Driver for WiFi," http://madwifi-project.org/.

[33] J. Lee, H. Lee, Y. Yi, S. Chong, B. Nardelli, E. W. Knightly, and M. Chiang, "Maing 802.11 DCF near-optimal: Design, implementation, and evaluation," 2012. [Online]. Available: http://lanada.kaist.ac.kr/ODCF.pdf

[34] M. J. Neely, "Super-fast delay tradeoffs for utility optimal fair scheduling in wireless networks," in *Proc. IEEE INFOCOM*, 2006.